

Three-dimensional Two-Layer Outer Gap Model: the Third Peak of Vela Pulsar

Y. Wang, J Takata & K.S. Cheng

Department of Physics, University of Hong Kong, Pokfulam Road, Hong Kong

We extend the two-dimensional two-layer outer gap model to a three-dimensional geometry and use it to study the high-energy emission of the Vela pulsar. We apply this three-dimensional two-layer model to the Vela pulsar and compare the model light curves, the phase-averaged spectrum and the phase-resolved spectra with the recent *Fermi* observations, which also reveals the existence of the third peak between two main peaks. The phase position of the third peak moves with the photon energy, which cannot be explained by the geometry of magnetic field structure and the caustic effect of the photon propagation. We suggest that the existence of the third peak and its energy dependent movement results from the azimuthal structure of the outer gap.

I. INTRODUCTION

The *Fermi*'s observation of the Vela Pulsar [1] shows that, in its light curve, as the energy increases, a third peak appears at the trailing part of the first peak and shifts towards the second peak, which makes this known γ -ray pulsar before *Fermi*'s era more special.

We want to use our two-layer Outer Gap model [2] to explain the strange third peak and its movements. Our two-dimensional two-layer model has explained the phase averaged spectra of the mature pulsars, including the Vela pulsar, in the first catalogue of γ -ray pulsars of *Fermi* [3]. However, to study the pulse profile, a three-dimensional model is needed. Therefore, we extend the two-layer model to a three-dimensional magnetic field. Here we present our simulations of the energy dependent light curves and the explanation of the moving third peak of Vela Pulsar, by three-dimensional two-layer Outer Gap model.

II. THE THREE-DIMENSIONAL TWO-LAYER OUTER GAP

In this study, the three-dimensional rotating vacuum dipole field is adopted. The γ -ray emissions come from the region with strong accelerating electric field, which extends above the last-open field lines and between the null charge surface of the Goldreich-Julian charge density [4] and the light cylinder. This region has a two-layer structure. As shown in Figure 1, in the trans-field direction of the magnetic field, the outer gap can be divided into two parts:

- 1 the main acceleration region at the lower part of the outer gap, where the charge density is assumed to be $\sim 10\%$ of the Goldreich-Julian value and a strong electric field is accelerating the particles to emit GeV photons via the curvature process,
- 2 the screening region around the upper boundary, where the growth of the main acceleration

region in the trans-field direction is stopped by the pair-creation processes.

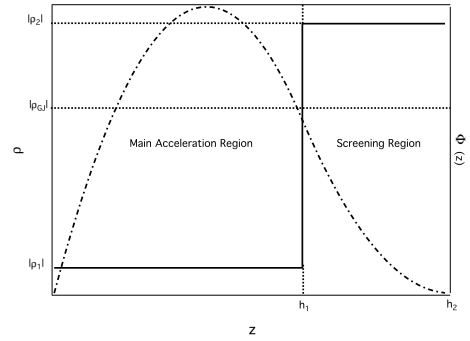


FIG. 1: The simplified distribution of the charge density (solid line) and the corresponding accelerating potential (dot-dashed line) of the two-layer outer gap.

And we use a simple step function to approximate the distribution of the charge density in the trans-field direction in the poloidal plane (the plane where the field lines have same polar angle ϕ_p) as

$$\rho(x, z, \phi_p) = \begin{cases} \rho_1(x, \phi_p), & \text{if } 0 \leq z \leq h_1(x, \phi_p) \\ \rho_2(x, \phi_p), & \text{if } h_1(x, \phi_p) < z \leq h_2(x, \phi_p) \end{cases}, \quad (1)$$

where x , z and ϕ_p represent coordinates along the magnetic field line, the height measured from the last-open field line, and the azimuthal direction. In addition, h_1 and h_2 represent the thickness of the main accretion region and the total gap thickness, respectively.

Instead of solving the real three-dimensional Poisson equation, we divide the gap into many equal divisions in the azimuthal direction and regard each slice of the gap as a two-dimensional two-layer gap. For each division, the solution of the potential in our two-dimensional study is applied. The shape of the γ -ray spectrum of the division is determined by three parameters: f , fractional gap thickness, h_1/h_2 , ratio of the thicknesses of the primary and whole region, and ρ_1 , the number density in the main acceleration region.

We define the gap fraction f measured on the stellar surface as [2],

$$f \equiv \frac{h_2(R_s)}{r_p}, \quad (2)$$

where R_s is the stellar radius, and $r_p(\phi_p)$ is the polar cap radius. The accelerating electric field $E_{||}$ is proportional to f^2 .

The accelerating electric is caused by the deviation of the charge density from the Goldreich-Julian charge density, so we introduce a parameter g to represent this deviation, the g and ρ satisfy the relation, $\rho(x, z, \phi_p) - \rho_{GJ}(x, \phi_p) \sim g(z, \phi_p)\rho_{GJ}(x, \phi_p)$. For each slice of the gap, the deviations of the charge density in the two region, $-g_1$ and g_2 , and h_1/h_2 satisfy

$$\left(\frac{h_2}{h_1}\right)^2 = 1 + \frac{g_1}{g_2}. \quad (3)$$

III. SIMULATION OF THE ENERGY DEPENDENT LIGHT CURVES

The first step is to determine the viewing angle and the inclination angle by making the ‘geometry determined’ light curve, whose peaks are due to the caustic effect and almost do not dependent on the energy. Our two-dimensional study shows that the fractional size of the gap is small (around 0.16), therefore, in this study, we trace the magnetic field lines of $a = 1 \rightarrow 0.93$. The factor a is used to represent the magnetic field lines at a given layer, where $a = 1$ and $a = 0$ represent the last-open field lines and magnetic axis, respectively.

The emission direction is calculated in observer’s frame [5]. The curvature photon is assumed to be emitted in the direction of the particle motion, which can be described as an combination of the motion along the magnetic field line and the drift motion,

$$\vec{v} = v_p \vec{B}/B + \vec{r} \times \vec{\Omega}, \quad (4)$$

where v_p is calculated from the condition that $|\vec{v}| = c$. The polar angle to the rotation axis ζ of the emission direction and the pulse phase ψ are calculated from [6]

$$\begin{cases} \cos \zeta = v_z/v \\ \psi = -\cos^{-1}(v_x/v_{xy}) - \vec{r} \cdot \vec{v}/R_L \end{cases} \quad (5)$$

If a point in a field line satisfies $|\zeta - \beta| < \varphi(r)$, the radiation of that point can be seen by the observer, where β is the viewing angle and $\varphi(r)$ is the solid angle of the radiation.

We find that the set of $(\alpha, \beta, a_{min}) = (57^\circ, 80^\circ, 0.935)$ reproduces right peak separation of the two peaks. Figure 2 shows the skymap of the emitted photons from the magnetic surface of $a = 0.95$ with $\alpha = 57^\circ$ and $\beta = 80^\circ$.

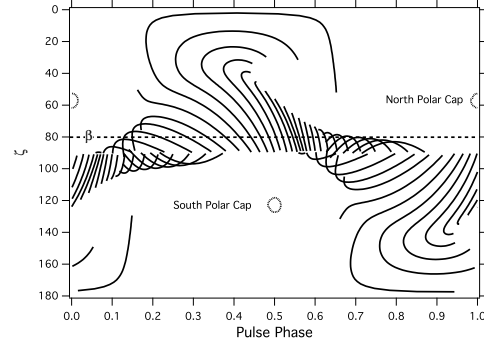


FIG. 2: The skymap of the radiations outside the null charge surface with inclination angle $\alpha = 57^\circ$. The x -axis is the pulse phase and the y -axis is the direction of the radiation. The dashed line is the viewing angle, which is chosen as $\beta = 80^\circ$.

Then we calculate the γ -ray spectrum to find proper values of the three parameters, $1 - g_1$, h_1/h_2 and f . We find that the values of these three parameters used in the two-dimensional study can provide a good spectrum. Here we assume the distance to the pulsar is 325 pc.

At last, we calculate the phase resolved spectra under the parameters found above, and integrate the phase resolved spectra to obtain the energy dependent light curves. The number of the photons measured at pulse phases between ψ_1 and ψ_2 is calculated from

$$N_\gamma(E_1, E_2, \psi_1, \psi_2) \propto \int_{E_1}^{E_2} F_{tot}(E, \psi_1 \leq \psi \leq \psi_2) dE, \quad (6)$$

where the F_{tot} is the phase resolved spectrum.

The calculated pulse profile under constant values of the three parameters in azimuthal direction can not explain the existence of the observed third peak. The fact that the simple caustic model can not explain the phase shift of the observed third peak, forces us to consider more complex structure of the emission region.

By the definition of f in equation (2), we may choose the form of the azimuthal distribution of f as,

$$f(\phi_p) = \frac{C}{r_p(\phi_p)}, \quad (7)$$

where the $C = 0.18 r_p^{max}$, r_p^{max} is the maximum value of the polar cap radius, and the factor 0.18 is chosen by fitting the phase averaged-spectrum.

It is expected that as the null charge surface is closer to the stellar surface, the number density of the X-ray photons increases in the gap and the screening region becomes thinner due to higher pair creation rate. Therefore, we assume the formula of the ratio as

$$\frac{h_1}{h_2}(\phi_p) = B_1 + B_2 \frac{1/r_{null}(\phi_p) - 1/r_{null}^{max}}{1/r_{null}^{min} - 1/r_{null}^{max}}, \quad (8)$$

TABLE I: The effects of the distributions of the three parameters

$f(\phi_p)$	$h_1/h_2(\phi_p)$	$\rho_1(\phi_p)$ ($1 - g_1$)	The Bump $0.1\text{GeV} < E < 1\text{GeV}$	The Third Peak $1\text{GeV} < E < 8\text{GeV}$	The Third Peak $8\text{GeV} < E < 20\text{GeV}$
0.2	0.927	0.05	no	no	no
0.2	Equation 8	0.05	phase $\sim 0.2 - 0.3$	no	no
0.2	0.927	Equation 3 & 9	no	phase ~ 0.26	phase ~ 0.26
Equation 7	0.927	0.05	no	no	phase ~ 0.4
Equation 7	Equation 8	Equation 3 & 9	phase $\sim 0.2 - 0.3$	phase ~ 0.26	phase ~ 0.33

By fitting the spectral shape, we obtain $B_1 = 0.89$ and $B_2 = 0.09$.

With the two-dimensional two-layer model, we found that the phase-averaged spectra for most of the γ -ray pulsars can be reproduced by the averaged charge density of $\bar{\rho}_0 \equiv [h_1\rho_1 + (h_2 - h_1)\rho_2]/h_2 \sim 0.5$. In three-dimensional magnetosphere, the actual $E_\perp(\phi_p)$ can make the particles in different ϕ_p -cell to drift into other ϕ_p -cell via the effect of $E_\perp \times B$. As a result, the actual average density is

$$\bar{\rho}(\phi_p) = \bar{\rho}_0 \frac{f(\phi_p + \Delta\phi_p)}{f(\phi_p)}, \quad (9)$$

where the $\bar{\rho}(\phi_p) = N(\phi_p)/f(\phi_p)$ is used and $\bar{\rho}_0 = 0.5$ is the averaged charge density without drift motion. Using the relationship between g_1 , g_2 and h_1/h_2 given by equation (3), the distribution of $1 - g_1$ can be obtained.

We expected that the particles' displacement due to the drift motion becomes more important on the magnetic field line that has a smaller radial distance to the null charge surface, because the particles run longer distance in the outer gap. To take into this effect, we assume the formula of displacement as

$$\Delta\phi_p = F \frac{1/r_{\text{null}}(\phi_p) - 1/r_{\text{null}}^{\text{max}}}{1/r_{\text{null}}^{\text{min}} - 1/r_{\text{null}}^{\text{max}}}, \quad (10)$$

where F is a fitting parameter, which is chosen as -28° .

Table I summaries the effects of the distributions of the parameters on the energy dependent light curves. Figure 3 shows the pulse profiles calculated by taking into account the azimuthal distributions f , h_1/h_2 and $1 - g_1$. The corresponding phase averaged spectrum is shown in Figure 4. Figure 5 is the intensity map in the pulse phase and the energy plane. The color represents the scaled number of the photons at the certain interval of the pulse phase. We find a moving third peak from the results.

We also fit the calculated phase resolved spectra with power law plus exponential cut-off form. Figure 6 shows the cut-off energy and the photon index, as functions of the pulse phase.

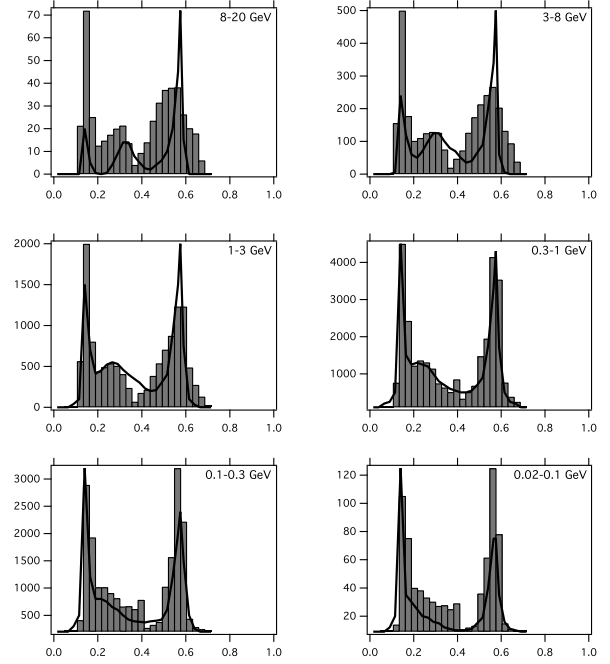


FIG. 3: The energy dependent light curves (histogram) with the distributions of $1 - g_1$, h_1/h_2 and f , provided by the three-dimensional outer gap. The solid lines are the observed light curves from Fermi-LAT [1].

IV. THE REASON FOR THE THIRD PEAK

The reason for the third peak and its shift is as follows. In the light curves, when energy lower than 1 GeV, the distributions of the thickness ratio h_1/h_2 makes a third-peak structure at ~ 0.2 pulse phase, because h_1/h_2 affects the emissivity in the screening region, which mainly produces the curvature photons of the energy less than 1 GeV. In the energy bands higher than 1 GeV, on the other hand, the azimuthal distributions of the fractional thickness, f , and the number density, $1 - g_1$, are more important, and they produce the third peak at $\sim 0.3 - 0.35$ pulse phase by providing higher electric field and more particles, respectively. Consequently, the differences in the standing phases of the third peak due to the distributions

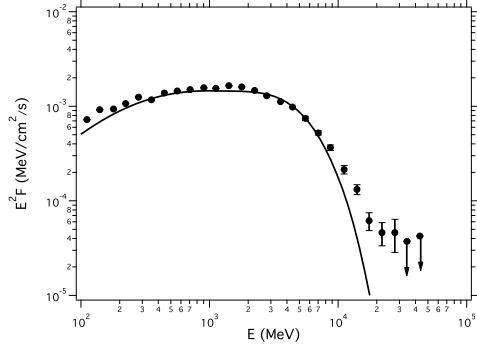


FIG. 4: The phase averaged spectrum with the distributions of $1 - g_1$, h_1/h_2 and f , comparing with the observed data (circle) from Fermi-LAT [1]

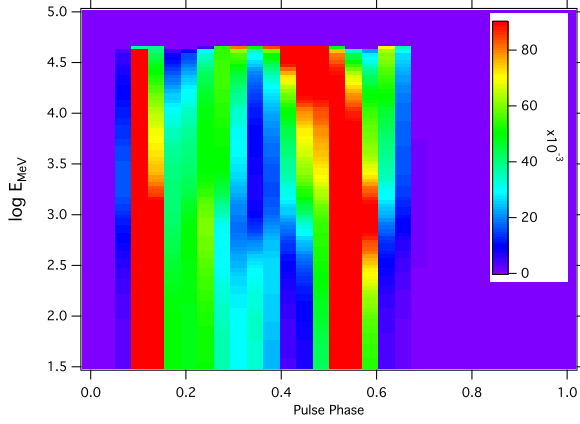


FIG. 5: Intensity map in the pulse phase and energy plane. The color represents the percentage of the number of the photons of certain interval of pulse phase in the total number of photons of certain interval of energy.

of h_1/h_2 , f and ρ_1 (or $1 - g_1$) produce the shift of the third peak with the photon energy.

Why is the Vela Pulsar so special? This is because: 1) It has a thin gap to make sure that its observable radiation contains both the contributions of the two layers. 2) Its γ -ray radiation is dominated by curvature photons that keep the effects of azimuthal structure of the gap visible. 3) Two-dimensional study shows that the shape of the spectrum is very sensitive to $\rho_1(\phi_p)$

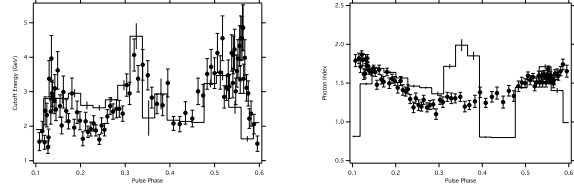


FIG. 6: The cutoff energies and photon indices of the phase-resolved spectra of different pulse phases, comparing with the observed data (circle) [1].

and $\frac{h_1}{h_2}(\phi_p)$, when ρ_1 and h_1/h_2 get close to 0 and 1, respectively. This makes the effects of azimuthal structure of the gap obvious. 4) The inclination angle also determines the azimuthal structure of the gap.

V. CONCLUSION

The third peak of Vela Pulsar can not be explained by the caustic effect determined by the magnetic field structure. This peak is due to the azimuthal distributions of the fractional gap thickness (f), the ratio of the thicknesses of the primary and whole region (h_1/h_2), and the number density in the main acceleration region (ρ_1). The distributions of ρ_1 and f make third-peak-like structure in the bridge region of light curve above 1 GeV, while the distribution of h_1/h_2 makes a bump in the bridge region of the light curves below 1 GeV. The phases of the third peaks caused by the azimuthal distributions of h_1/h_2 , ρ_1 and f are different from each other. Consequently, the differences in the phases produce the shift of the combined third peak with the photon energy.

Acknowledgments

We thank L. Zhang for useful discussion. This work is supported by a GRF grant of the the Hong Kong SAR Government entitled ‘‘Gamma-ray Pulsars’’ (HKU700911P).

[1] Abdo A.A. et al., 2010, ApJ, 713, 154
 [2] Wang Y., Takata J. & Cheng K. S., 2010, ApJ, 720, 178
 [3] Abdo A.A. et al., 2010, ApJS, 187, 460
 [4] Goldreich P. & Julian W.H., 1969, ApJ, 157, 869

[5] Takata J., Chang H.-K. & Cheng K.S., 2007, ApJ, 656, 1044
 [6] Yadigaroglu I. A., 1997, Ph.D. thesis, Stanford Univ.